Identification of Ubiquilin, a Novel Presenilin Interactor That Increases Presenilin Protein Accumulation

Alex L. Mah,* George Perry,‡ Mark A. Smith,‡ and Mervyn J. Monteiro*

*Medical Biotechnology Center, Department of Neurology, University of Maryland Biotechnology Institute, Baltimore, Maryland 21201; and ‡Institute of Pathology, Case Western Reserve University, Cleveland, Ohio 44106

Abstract. Mutations in the highly homologous presenilin genes encoding presenilin-1 and presenilin-2 (PS1 and PS2) are linked to early-onset Alzheimer's disease (AD). However, apart from a role in early development, neither the normal function of the presenilins nor the mechanisms by which mutant proteins cause AD are well understood. We describe here the properties of a novel human interactor of the presenilins named ubiquilin. Yeast two-hybrid (Y2H) interaction, glutathione *S*-transferase pull-down experiments, and colocalization of the proteins expressed in vivo, together with coimmunoprecipitation and cell fractionation studies, provide compelling evidence that ubiquilin interacts with both PS1 and PS2. Ubiquilin is noteworthy since it contains multiple ubiquitin-related domains typically thought to be involved in targeting proteins for degradation. However, we show that ubiquilin promotes presenilin protein accumulation. Pulse-labeling experiments indicate that ubiquilin facilitates increased presenilin synthesis without substantially changing presenilin protein half-life. Immunohistochemistry of human brain tissue with ubiquilin-specific antibodies revealed prominent staining of neurons. Moreover, the anti-ubiquilin antibodies robustly stained neurofibrillary tangles and Lewy bodies in AD and Parkinson's disease affected brains, respectively. Our results indicate that ubiquilin may be an important modulator of presenilin protein accumulation and that ubiquilin protein is associated with neuropathological neurofibrillary tangles and Lewy body inclusions in diseased brain.

Key words: presenilins • Alzheimer's disease • ubiquilin • ubiquitin • proteasome

Introduction

Alzheimer's disease (AD)[1] is a progressive neurodegenerative disorder characterized by impaired memory and cognition, as well as altered behavior. The majority of AD cases are late-onset, appearing in people over the age of 65. However, a small percent (~5%) of cases, termed early-onset, arise at an unusually young age, as early as the third decade of life. Molecular genetic analysis has linked early-onset familial Alzheimer's disease (FAD) to the autosomal dominant inheritance of mutations in three genes: the β-amyloid precursor protein (APP) and two homologous genes, presenilin-1 and -2 (PS1 and PS2) (Hardy, 1997; Price et al., 1998). The mechanisms by which mutations in these three genes cause AD are unresolved.

PS1 and PS2 are multitransmembrane proteins that share 67% sequence identity. The topology of presenilins is debatable, though the most widely drawn models show proteins that weave through the membrane eight times, with the NH_2- and COOH-terminal domains and a large "loop" between transmembrane domains six and seven all oriented towards the cytoplasm (see Fig. 1 A) (Haass and De Strooper, 1999). Although both proteins share extensive sequence identity along their entire lengths, their NH_2-terminal domains and the second half of their loops are highly divergent, suggesting that these unique regions could modulate different functions of the two presenilins. An examination of presenilin-linked FAD mutations mapped so far reveals that most are missense mutations in identical residues spread throughout the polypeptide in both presenilins, suggesting that the conserved residues are important for the function of the proteins.

Studies of presenilin homologues in various species have indicated that presenilin genes are required for proper development. Mutation of the *Caenorhabditis elegans* presenilin gene, *sel-12*, produces defects in vulva development linked to cell signaling defects involving Notch-based re-

Address correspondence to Mervyn J. Monteiro, Medical Biotechnology Center, Room N352, 725 West Lombard Street, Baltimore, MD 21201. Tel.: 410-706-8132. Fax: 410-706-1732. E-mail: monteiro@umbi.umd.edu

[1]*Abbreviations used in this paper:* aa, amino acid; AD, Alzheimer's disease; APP, β-amyloid precursor protein; EST, expressed sequence tag; FAD, familial Alzheimer's disease; GFP, green fluorescent protein; NFT, neurofibrillary tangles; ORF, open reading frame; PD, Parkinson's disease; PS, presenilin; RACE, rapid amplification of cDNA ends; UB, ubiquitin; UBA, ubiquitin-associated; Y2H, yeast two-hybrid.

ceptors (Levitan and Greenwald, 1995; Haass and De Strooper, 1999). Disruption of the *Drosophila melanogaster* presenilin gene results in embryonic lethality, with embryos displaying severe Notch-like phenotypes (Struhl and Greenwald, 1999; Ye et al., 1999). Mammalian presenilins also play important roles in early development, as disruption of the mouse PS1 gene leads to death shortly after birth, with embryos displaying central nervous system defects together with abnormal patterning of the axial skeleton and spinal ganglia (Shen et al., 1997; Wong et al., 1997). Interestingly, $PS1^{-/-}$ mice can be rescued by a human transgenes containing FAD-linked mutations, indicating that the FAD mutations do not affect presenilin functions related to embryo development (Davis et al., 1998; Qian et al., 1998). In contrast, disruption of the mouse PS2 gene produces no obvious defects, but PS1/PS2 double knock-out mice die earlier at embryonic day 9.5 and, like $PS1^{-/-}$ mice, display severe misexpression of proteins involved in Notch signaling (Donoviel et al., 1999; Herreman et al., 1999). These results indicate that there is functional redundancy between PS1 and PS2; PS1 can compensate for PS2, but PS2 cannot compensate for PS1, at least during early mouse development.

Both human presenilin genes are ubiquitously expressed, but at low levels. In brain the proteins are more highly expressed in neurons than glia (Price et al., 1998). Knowledge of where presenilin proteins localize in cells is important for understanding their function. However, uncertainties exist regarding their precise subcellular localization. In neurons, endogenous PS1 and PS2 have been localized to the ER and to vesicular structures of the somatodentritic compartment and axons (Price et al., 1998; Haass and De Strooper, 1999). When overexpressed, the proteins predominantly localize to the ER, the Golgi complex, and the nuclear envelope (Kovacs et al., 1996; Janicki and Monteiro, 1997; Haass and De Strooper, 1999). However, in nonneuronal cells, endogenous presenilins have been localized to the ER, Golgi complex, centrosomes, centromeres, and cell surface (Georgakopoulos et al., 1999; Haass and De Strooper, 1999; Raina et al., 1999). It is not known to what extent these diverse locations reflect true sites of presenilin function.

The presenilin proteins have been linked to several cellular functions. Interestingly, some of these cellular functions are compromised or altered by the expression of PS genes containing FAD mutations. The presenilin proteins have been shown to play important roles in apoptosis, calcium homeostasis, cell cycle regulation, regulation of misfolded proteins in the ER, and cleavage of APP (Guo et al., 1997; Janicki and Monteiro, 1997, 1999; Cotman, 1998; Mattson et al., 1998; Haass and De Strooper, 1999; Katayama et al., 1999; Leissring et al., 1999; Niwa et al., 1999). Further clues regarding presenilin functions are emerging from a growing list of proteins with which presenilin interacts. Previously, we identified and characterized calmyrin, a newly discovered calcium-binding protein, which preferentially interacts with the PS2 loop and modulates presenilin-induced cell death (Stabler et al., 1999). Here, we describe a novel human presenilin-interacting protein, which we have named ubiquilin. We describe evidence that indicates ubiquilin modulates presenilin protein levels and is associated with neuropathological lesions such as NFTs and Lewy bodies in AD and PD affected brains.

Materials and Methods

Ubiquilin cDNA and Protein Sequences

The GenBank/EMBL/DDBJ ubiquilin cDNA accession number is AF176069, and the ubiquilin protein accession number is AAD49751 (see updated NM_013438).

Yeast Two-Hybrid Experiments

The yeast two-hybrid (Y2H) procedure that utilizes the LexA/transactivation system was performed, as described previously (Stabler et al., 1999). The PS2 COOH-terminal 39-amino acids (residues K410–I448) (see Fig. 1, A and B) were used as bait to screen a human fetal brain cDNA library. Out of $\sim 10^7$ primary yeast transformants, ~50 clones were selected for further analysis based on growth in the absence of leucine and a substantial blue color change when grown on 5-bromo-4-chloro-3-indolyl-β-D-galactopyranoside (X-gal) plates. False positives were subsequently eliminated based on their interactions with negative-control baits, such as LexA alone, nuclear lamin B, and CENP-C centromere protein. Plasmid DNAs were isolated from clones that fulfilled the above requirements, and the DNA sequences of their inserts were determined and compared with the GenBank/EMBL/DDBJ databases using the BLAST search program. Two of the interactors contained overlapping portions of the 3′ end of a novel human transcript, which we named ubiquilin. Interaction of ubiquilin proteins with various PS1 and PS2 baits were quantified in liquid culture assays by the enzymatic conversion of *o*-nitrophenyl-β-D-galactopyranoside (ONPG) to *o*-nitrophenol and D-galactose by β-galactosidase enzyme encoded by a Y2H reporter plasmid.

Rapid Amplification of cDNA Ends (RACE)

5′ RACE, using strategically designed ubiquilin-specific primers, was performed to obtain the full-length coding sequence of ubiquilin. The PCR reactions were carried out according to the instructions provided by the manufacturer, using an AP1 adaptor–ligated human adult brain cDNA library as template and the Advantage cDNA Polymerase Mix (CLONTECH Laboratories, Inc.). The procedure resulted in the isolation of 1,053 additional bps of the 5′ sequence, with respect to the longest original Y2H clone. The full-length ubiquilin open reading frame (ORF) was subsequently obtained by sequencing a human expressed sequence tag (EST) clone (American Type Culture Collection), which provided an extra 108 bps of 5′ sequence, including the ATG start codon, a Kozak consensus sequence, and an upstream in-frame stop codon. In addition, comparison of the sequence with the TIGR Tentative Human Consensus database returned another independent EST sequence (THC296552), which corroborated the ATG start codon.

Radiation Hybrid Mapping

A GeneBridge 4 radiation hybrid panel (Research Genetics) was performed with two ubiquilin gene-specific primers, RH1 (5′-GCAGCGACAACTTTTGTCTAACCCTG-3′) and RH2 (5′-CAGGCACCAAATTTGGCGCAGTAG-3′), and each of the 93 indexed human genomic DNA template pools. The conditions for the PCR reactions were similar to that of the 5′ RACE procedure, except that a longer initial denaturation step was used. Positive and negative reactions (1 or 0, respectively; 2 represents an ambiguous reaction) were compiled (0100010001 1002100110 0000011000 1011000000 1100000001 0010001001 0100010000 0111100000 1000000000 000), and the vector data was submitted to the Whitehead Institute/MIT Center for Genome Research website (http://carbon.wi.mit.edu:8000/cgi-bin/contig/rhmapper.pl) for comparison with their radiation hybrid database.

Northern Blot Analysis

cDNA hybridization probes were ^{32}P-radiolabeled by random primer labeling of ~100 ng of two ubiquilin cDNA restriction fragments, X (bases 1,132–1,860) and Y (bases 284–967), shown in Fig. 2 II. Each probe was hybridized to a different human mRNA Northern blot, Human Multiple Tissue Northern Blot I, and Human Brain MTN II, respectively (CLONTECH Laboratories, Inc.). After hybridization, the blots were washed twice with 2.0× SSC and 0.05% SDS at 50°C and then twice again with 0.1× SSC and 0.1% SDS at 50°C, before exposure to autoradiography film. Both blots were subsequently stripped in near-boiling temperature 0.5% SDS and then reprobed with radiolabeled human β-actin cDNA control probe (CLONTECH Laboratories, Inc.). The band intensities

were quantified using GelExpert 97 2.0 (Nucleotech Corp.), divided by the β-actin control band intensity from the same lane, and then normalized against the lowest value.

Bacterial Expression of Ubiquilin Proteins

To express full-length nonfusion ubiquilin protein in bacteria, an NcoI/XhoI cDNA fragment containing the entire ubiquilin ORF was subcloned into pET-15b (Novagen) and then transformed into *Escherichia coli* BL21(DE3). Ubiquilin protein expression was induced with 1.0 mM IPTG at 37°C for 2–3 h. Bacteria were lysed, and the protein extracts were separated by SDS-PAGE. Proteins were transferred onto nitrocellulose filters and immunoblotted with anti-ubiquilin pAb. In addition, various partial-length GST–ubiquilin fusion proteins were constructed, expressed, and purified using the GST-protein purification procedures described previously (Janicki and Monteiro, 1997). The specific subregions of ubiquilin that were expressed are depicted in Fig. 2 III.

Rabbit pAb Production and Affinity Purification

Rabbit anti-ubiquilin polyclonal antisera were generated against purified GST–ubiquilin fusion proteins B or C (Fig. 2 III) by Covance Research Products, Inc. Affinity-purified anti–ubiquilin-C antibodies were obtained by passing anti–C-serum first over a column containing GST alone coupled to CH-Sepharose 4B beads at 4°C overnight, to eliminate antibodies binding to GST, and then by mixing the flow-through fraction with ubiquilin–coupled CH-Sepharose 4B beads at 4°C overnight. After extensive washing, antibodies that bound to the ubiquilin-coupled beads were eluted dropwise with 0.1 M sodium citrate and 0.3 M sodium chloride solution, pH 2.2, and collected as ~240-μl fractions into tubes containing 40 μl 1 M Tris-HCl, pH 9.1, to restore neutral pH.

In Vitro Transcription and Translation

[^{35}S]Methionine-radiolabeled ubiquilin or luciferase proteins were synthesized in rabbit reticulocyte lysates with an in vitro transcription and translation system (Promega) at 30°C for 90 min. [^{35}S]Methionine-radiolabeled PS2 and PS1 were synthesized using the same system, but with the addition of canine pancreatic microsomal membranes (Promega) during transcription and translation.

GST Pull-down Binding Assay

Various purified GST–ubiquilin fusion proteins already bound to glutathione-agarose beads were incubated with ~2.5 μl [^{35}S]methionine-radiolabeled presenilin protein, in addition to protease inhibitors and 0.8% BSA at 4°C for 1 h with rocking. The beads were washed several times with pull-down buffer (0.5% NP-40 in 1.0× PBS), once with 200 mM KCl in pull-down buffer, and several more times with pull-down buffer alone. Supernatants and washes were discarded, whereas the bound proteins on the beads were mixed with sample loading buffer (Janicki and Monteiro, 1999) and separated by SDS-PAGE. Then, the gel was stained with Coomassie blue to ensure equal loading of GST–ubiquilin fusion proteins. The gels were dried and exposed to autoradiography film.

Mammalian Expression and Fusion Constructs

Full-length ubiquilin was expressed using the pGEM-CMV mammalian expression vector (Janicki and Monteiro, 1997) (see Fig. 2 IV). In addition, two ubiquilin fusion proteins were constructed within the same expression vector. In one, green fluorescent protein (GFP) was fused to the NH_2 terminus of ubiquilin (beginning at residue 20 [Ala]), whereas in the other, a myc epitope tag was fused to the COOH terminus of full-length ubiquilin.

HeLa Cell Culture and DNA Transfection

HeLa cells were grown at 37°C in DME supplemented with 10% FBS and transfected with plasmid DNAs, using the calcium phosphate coprecipitation method.

Western Blot Analysis

Cells were lysed in buffer containing protease inhibitors (Monteiro and Mical, 1996), and protein concentrations were determined by the bicinchonic acid (BCA) assay. Lysates containing known amounts of protein were mixed with sample loading buffer (Janicki and Monteiro, 1999) and either heated at 100°C for 5 min or at 37°C for 15 min before separation by SDS-PAGE. The 37°C incubation was used to detect presenilin proteins by minimizing their tendency to aggregate and resist entry into the gels. After gel electrophoresis, proteins were transferred onto nitrocellulose filters and immunoblotted according to procedures described previously (Janicki and Monteiro, 1997). In addition to our own rabbit anti-ubiquilin antibodies, we also used the following primary antibodies: goat anti-PS1, anti-PS2, and anti-BiP (NH_2 terminus specific; Santa Cruz Biotechnology, Inc.); rabbit anti-PS2 (NH_2 terminus or loop specific, raised to the corresponding GST–PS2 fusion proteins) (Janicki and Monteiro, 1997, 1999) anti-ubiquitin (Dako), anti-lamin A/C (Mical and Monteiro, 1998), anti-calnexin, and anti-calreticulin (StressGen); and mouse anti-GFP (Zymed Laboratories), anti–α-tubulin (Sigma-Aldrich), and anti-lamin B (Matri-Tect). Binding of primary antibodies were detected with ^{125}I-protein A or by incubation with appropriate secondary horseradish peroxidase–conjugated antibodies (New England Biolabs, Inc.) using autoradiography or chemiluminescence, respectively.

Immunoprecipitation and Cell Fractionation Studies

HeLa cells, 17 h after transfection with PS2 plasmid DNA, were collected in immunoprecipitation buffer (50 mM Tris-HCl, pH 7.5, 150 mM NaCl, 0.5% NP-40, 2 mM EDTA) and homogenized by gentle strokes with a Dounce homogenizer. After centrifugation, the pellet was discarded, and the proteins were immunoprecipitated from the remaining supernatant by adding rabbit antisera (preimmune, anti–PS2-NH_2 terminus, or anti–PS2-Loop) and protein A–Sepharose CL-4B beads (Stabler et al., 1999). The beads were recovered by centrifugation and washed with 0.5% NP-40 in 1.0× PBS. They were boiled in sample loading buffer, and the bound proteins were analyzed by SDS-PAGE and immunoblotting. Blots were probed with primary anti–ubiquilin-B antibodies, which were subsequently detected with ^{125}I-protein A. Soluble, insoluble, Triton X-100–soluble, and Triton X-100–insoluble protein fractions of untransfected or PS2-transfected HeLa cells were prepared according to the procedure described previously (Stabler et al., 1999). Equal amounts of each fraction were separated by SDS-PAGE and, after electroblot transfer to nitrocellulose filters, were immunoblotted with either affinity-purified anti–ubiquilin-C antibody, anti–PS2-NH_2 terminus antibody, or anti-lamin A/C antibody (Mical and Monteiro, 1998). The partitioning of endogenous lamin A/C proteins was monitored, since their cell fractionation behavior was known (Mical and Monteiro, 1998; Stabler et al., 1999).

Cell Staining and Immunofluorescence Microscopy

The procedure used for immunofluorescence staining of HeLa cells was described previously (Janicki and Monteiro, 1997). Indirect immunofluorescent microscopy, digital image capture, and subsequent manipulation and merging of images were done with a Leica DM IRB microscope attached to a PowerMac computer running Signal Analytics IPLab Spectrum software (Stabler et al., 1999). Confocal images were captured on a Axiovert 100 microscope using LSM software (ZEISS). The primary antibodies used were: rabbit anti–ubiquilin-B and affinity-purified anti–ubiquilin-C, goat anti-PS1 and anti-PS2 (NH_2 terminus specific) (Santa Cruz Biotechnology, Inc.), and mouse anti-myc (Mical and Monteiro, 1998).

Human Brain Immunohistochemistry

Hippocampus brain tissue from six AD cases (aged 77–95) and five control cases (aged 19–71) were fixed in methacarn (6:3:1, chloroform/methanol/acetic acid) overnight. Locus coreuleus or substantia nigra brain tissue from three PD cases (aged 53–66) were fixed in formalin overnight, whereas frontal cortex brain tissue from two cases of diffuse Lewy body disease (aged 49 and 85) were fixed in either formalin or methacarn overnight. Samples were dehydrated and embedded in paraffin. Sections were cut 6-μm thick and mounted onto glass slides. After deparaffinization with xylene, sections were hydrated through graded ethanol treatment, and the endogenous peroxidase activity was eliminated by incubation in 3% hydrogen peroxide for 30 min. Nonspecific binding sites were blocked with 10% normal goat serum in Tris-buffered saline (50 mM Tris-HCl, 150 mM NaCl, pH 7.6) for 30 min before application of either preimmune sera, affinity-purified anti–ubiquilin-C antibody, or anti–ubiquilin-B antibody. Immunostaining was performed using the peroxidase–anti-peroxidase method, with DAB as cosubstrate (Sternberger, 1986). Color images of the stained slides were captured using a Sony Digital Photo Camera DKC-5000 on a Nikon Eclipse E600 microscope using Adobe Photoshop® software.

Protein Accumulation Studies

HeLa cells were transfected with expression constructs encoding ubiquilin protein (15 μg plasmid DNA), PS2 protein (7 μg plasmid DNA), or both. At 12 h after transfection, the cells were incubated for an additional 5–6 h in DME/FBS media in the absence or presence of proteasome inhibitors (20 μM synthetic lactacystin or 40 μM MG-132; Calbiochem-Novabiochem). Afterwards, the cells were lysed in buffer containing protease inhibitors and the protein concentrations were determined. Protein extracts totaling 100 μg were loaded per lane, separated by SDS-PAGE, and immunodetected with various antibodies. In a follow up experiment, HeLa cells were cotransfected with a constant amount of PS2 (7 μg plasmid DNA) and increasing amounts of either ubiquilin (0, 1, 2, 3, and 4 μg plasmid DNA) or GFP (0, 1, 2, 3, and 4 μg plasmid DNA) expression vectors.

Pulse-Chase Experiments

Exponentially growing HeLa cells maintained in flasks were trypsinized and resuspended at a density of 2.68×10^6 cells/ml in Opti-MEM medium (GIBCO BRL). Two 0.5-ml aliquots of the cell suspension were each electroporated with a mixture of either 7 μg PS2 and 15 μg of EGFP-C1 (CLONTECH Laboratories, Inc.) expression plasmid DNA or 7 μg PS2 and 15 μg of ubiquilin expression plasmid DNA. The aliquots containing the same DNA mixture were then combined, resuspended in 28 ml of OptiMEM medium (containing 10% FBS), and 2 ml of the suspension was plated in 14 separate wells (9.5 cm^2). The cells were incubated for 7 h to allow for attachment to the dishes, and then the medium was removed and replaced with DME containing 10% FBS. Incubation was continued for an additional 14 h. The cells were starved for 45 min in methionine-deficient DME containing 10% dialyzed FBS. The medium was removed and the cells in each well were pulse labeled by adding 1 ml of the methionine-deficient medium containing 150 μCi of [^{35}S]methionine (1,000 Ci/mmol; Amersham Pharmacia Biotech) for 1 h. After labeling, the cells were washed twice with DME containing 1 mM nonradioactive L-methionine and 10% dialyzed FBS, and then they were chased with 2 ml of the same medium for 0–6 h. At appropriate time intervals, the cells were washed three times with ice-cold 1.0× PBS and lysed in buffer containing protease inhibitors (Monteiro and Mical, 1996). The lysates were diluted 10-fold with immunoprecipitation buffer before PS2 proteins were immunoprecipitated, which was done by the addition of 5 μl rabbit anti-loop PS2 antibody (directed against GST-PS2 loop purified protein) (Janicki and Monteiro, 1997) and 100 μl of a slurry of protein A–Sepharose (Amersham Pharmacia Biotech). The immunoprecipitated proteins attached to the Sepharose beads were eluted by incubation with protein sample loading buffer (lacking SDS), which contained 8 M urea, 10 mM DTT, and 10% β-mercaptoethanol (Janicki and Monteiro, 1999), at 37°C for 15 min. The entire volume of samples were separated by SDS-PAGE on 8.5% gels. After electrophoresis, the gel was stained with Coomassie blue, impregnated with 2,5-diphenyloxazole, and dried (Stabler et al., 1999). The radioactivity of the immunoprecipitated PS2 band in each lane, corresponding to full-length PS2 protein, was quantified using a Molecular Dynamics Storm 840 Phosphoimager using ImageQuant software (Molecular Dynamics).

The half-life of endogenous HeLa ubiquilin protein was estimated by pulse labeling mock-electroporated HeLa cells for 1 h with 100 μCi of [^{35}S]methionine, followed by a chase with nonradioactive medium for 0–21 h. Ubiquilin protein was immunoprecipitated using 5 μl of rabbit anti–ubiquilin-C antibody, and the amount of radioactivity incorporated in the ubiquilin bands was determined after SDS-PAGE and phosphoimage analysis.

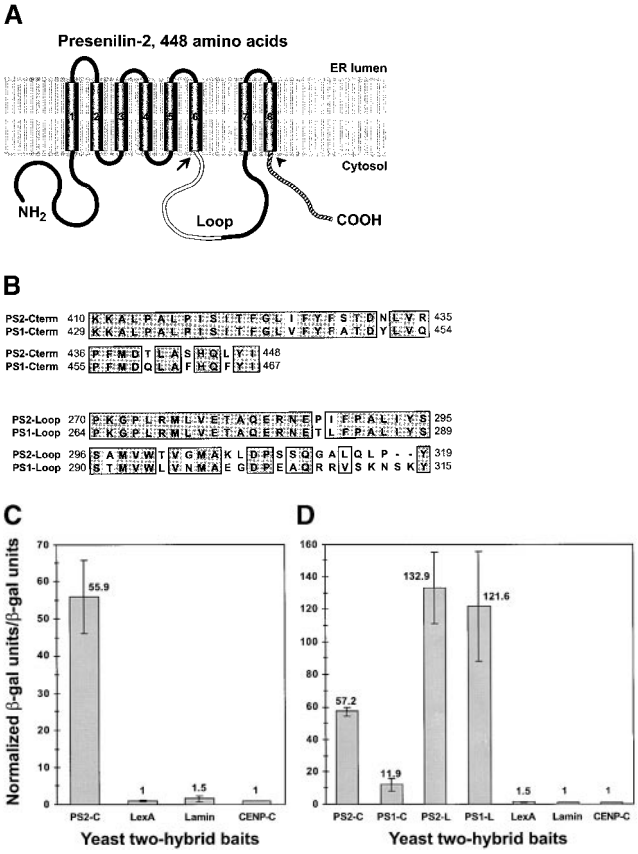

Figure 1. Ubiquilin interacts with two different regions of presenilin proteins. (A) A schematic diagram of ER-bound human PS2 and shows eight transmembrane domains with its NH_2 terminus, large hydrophilic loop, and COOH terminus all protruding into the cytoplasm. PS1 is believed to have a similar structure. The presenilin loop region (Loop, in white) and COOH terminus (striped) were used in Y2H assays. Two PS2 mutants used in this study contained progressively longer COOH-terminal deletions: PS2(ΔC), which terminated at the arrowhead, and PS2(ΔLC), which terminated at the arrow. (B) The amino acid sequence of PS1 and PS2 COOH terminus and loop regions that were used as Y2H baits. (C) Y2H β-galactosidase liquid culture interaction assay of an ubiquilin-prey clone (Fig. 2 III, construct B without GST) with PS2-COOH terminus (PS2-C), LexA alone, nuclear lamin B, and CENP-C baits. The β-galactosidase units were normalized to CENP-C, the bait with the weakest interaction. (D) β-Galactosidase interaction assay data of a near full-length ubiquilin-prey clone (Fig. 2 III, construct H without GST) repeated with the same baits described in C along with PS1-COOH (PS1-C) terminus, PS2-Loop (PS2-L), and PS1-Loop (PS1-L) baits. Again, β-galactosidase units were normalized to CENP-C.

Results

Identification of Human Ubiquilin, a Novel Interactor of the Presenilin Proteins

A novel human protein, which we named ubiquilin, for a protein with ubiquitin-related protein domains that interacts with the presenilins, was identified in a yeast two-hybrid screen (Y2H) for proteins that interact with the PS2 COOH-terminal sequence (Fig. 1, A and B). Two overlapping clones encoding the COOH-terminal 203 and 218 residues of ubiquilin were isolated in the screen. To clone the entire ubiquilin ORF, 5′ RACE was performed. This yielded 1,053 bps of additional upstream sequence, including an in-frame methionine codon located at the beginning of a ubiquitin-like (UB) domain. Conceptual translation from this methionine predicted a 559-amino acid protein. However, this methionine was unlikely to be the authentic start codon since translation from it produced a protein that was noticeably smaller, as seen by SDS-PAGE, than endogenous ubiquilin detected using pAb raised to the COOH-terminal 218 residues of ubiquilin (data not shown). Subsequent EST database searches and sequencing of putative overlapping clones yielded a clone with a longer 5′ end, which included an upstream in-frame methionine codon (corresponding to a 595-amino acid protein). Several lines of evidence indicate that this methionine codon was the au-

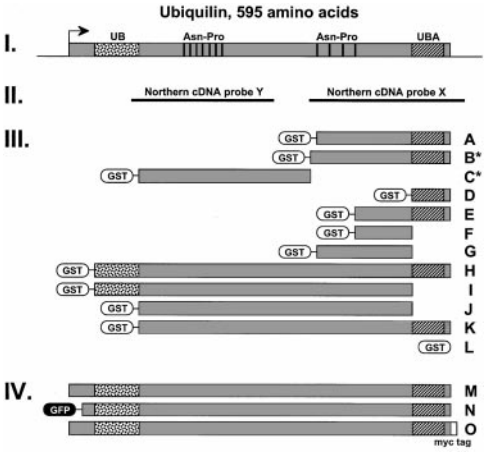

Figure 2. Schematic drawings of ubiquilin expression constructs. (I) The full-length ubiquilin polypeptide consists of 595 residues and contains an NH_2-terminal UB domain (speckled), a COOH-terminal UBA domain (striped), and several regularly spaced asparagine-proline (Asn-Pro) repeats (vertical bars). (II) The probes used in human Northern blots. (III) GST-fusion constructs: A (N393–S595 aa), B (Q378–S595 aa), C (Q113–M377 aa), D (Q541–S595 aa), E (D449–S595 aa), F (D449–L540 aa), G (N393–L540 aa), H (M37–S595 aa), I (M37–L540 aa), J (Q113–L540 aa), K (Q113–S595 aa), and L (GST alone). The ubiquilin portions of constructs A and B were isolated in the original Y2H screen. Bacterially expressed GST–fusion B and C polypeptides were used as immunogens for anti-ubiquilin pAb production (*). (IV) Mammalian expression constructs: M, full-length untagged ubiquilin; N, NH_2-terminal GFP-tagged ubiquilin fused at residue 20 (Ala); and O, COOH-terminal myc epitope-tagged ubiquilin.

thentic start methionine of ubiquilin. (a) This start methionine contained a Kozak consensus sequence and an upstream in-frame stop codon. (b) Polypeptides translated from this start codon matched the endogenous ubiquilin protein in size, which was 66 kD in HeLa and other human cell types. (c) Mammalian overexpression of the complete ubiquilin ORF (see Fig. 3, D–F), in vitro transcribed and translated ubiquilin in rabbit reticulocyte lysates (see Fig. 3 G), and human ubiquilin protein synthesized in bacteria (see Fig. 3 H) all generated 66-kD proteins. These data indicated that we had cloned the complete ubiquilin ORF and that the protein is probably not extensively modified in mammalian cells, since bacterially and eukaryotically expressed human ubiquilin proteins have similar molecular masses when separated by SDS-PAGE.

Interaction between ubiquilin and the presenilins was quantified in Y2H β-galactosidase liquid culture assays. A partial ubiquilin clone (encoding the COOH-terminal 218 residues), isolated from the Y2H screen, and a near full-length clone (encoding residues 37–595) both bound to the PS2-COOH-terminal bait >55-fold compared with negative-control baits (Fig. 1, C and D, respectively). However, the longer ubiquilin clone interacted less strongly with the PS1–COOH-terminal bait. This interaction nevertheless was still >12-fold compared with the negative-control baits (Fig. 1 D). We also tested whether ubiquilin would interact with portions of the loop regions of the presenilins (Fig. 1, A and B) that we had used in another Y2H study (Stabler et al., 1999). Interestingly, the near full-length ubiquilin construct also interacted well with both PS2 and PS1 loop sequences, and, surprisingly, the interaction was approximately twice as strong as with the PS2–COOH-terminal bait (Fig. 1 D). This suggested that two separate regions within the presenilin proteins could interact with ubiquilin.

The Gene for Ubiquilin Is Located on Chromosome 9q22 and Is Widely Expressed

Northern blot analysis of human tissues indicated that ubiquilin mRNA is widely expressed as a major 4.4-kb transcript, with several smaller differentially expressed minor

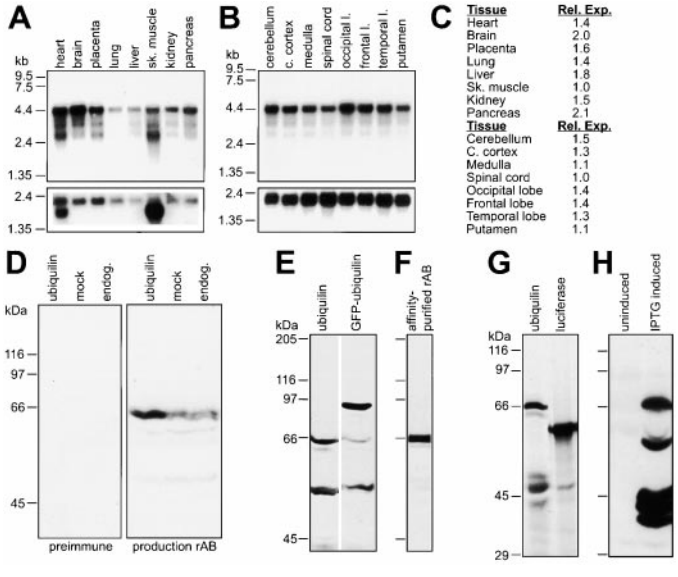

Figure 3. Ubiquilin mRNA and protein expression. (A) Human multiple tissue were analyzed by Northern blot and probed with ubiquilin cDNA fragment X (Fig. 2 II). After stripping, the blot was reprobed with a β-actin control fragment (shown below). (B) Northern blot of specific regions of the human brain probed with ubiquilin cDNA fragment Y (Fig. 2 II), with a reprobe with β-actin, which is shown below. (C) Quantification of ubiquilin mRNA expression levels. Relative expression of ubiquilin in different tissues was determined by densitometric analysis of the autoradiographs and relating the ubiquilin band intensities to the levels of β-actin hybridization from the same lanes. The values are presented after normalization against skeletal muscle (above) and spinal cord (below). (D–F) Characterization of anti-ubiquilin antibodies. Rabbit antibodies were raised against GST–ubiquilin fusion proteins B and C, generating anti-ubiquilin-B and anti–ubiquilin-C antibodies, respectively. (D) Anti–ubiquilin-B antibody was used to detect overexpressed and endogenous ubiquilin in ubiquilin transfected, mock-transfected, and untransfected (endogenous) HeLa cells. The anti–ubiquilin-B antibody detected a 66-kD doublet band, whereas preimmune sera did not. (E) Anti–ubiquilin-C antibody also recognized the 66-kD band in untransfected HeLa lysates and to varying extents a ~55-kD band. HeLa cells transfected with GFP–ubiquilin (Fig. 2 IV, N) contain an additional 93-kD reactive band, due to the fusion of the 27-kD moiety of GFP with ubiquilin. (F) Affinity-purified anti–ubiquilin-C antibody specifically reacts with the 66-kD band from transfected HeLa cell lysates. (G) Full-length in vitro transcribed and translated [^{35}S]methionine-radiolabeled human ubiquilin polypeptides migrated at 66 kD, whereas radiolabeled luciferase migrated at 61 kD. (H) Uninduced and IPTG-induced lysates of bacteria transformed with untagged full-length human ubiquilin and probed with anti–ubiquilin-B antibodies. Full-length immunoreactive ubiquilin (66 kD) and a series of smaller breakdown products are only seen in the induced lysate.

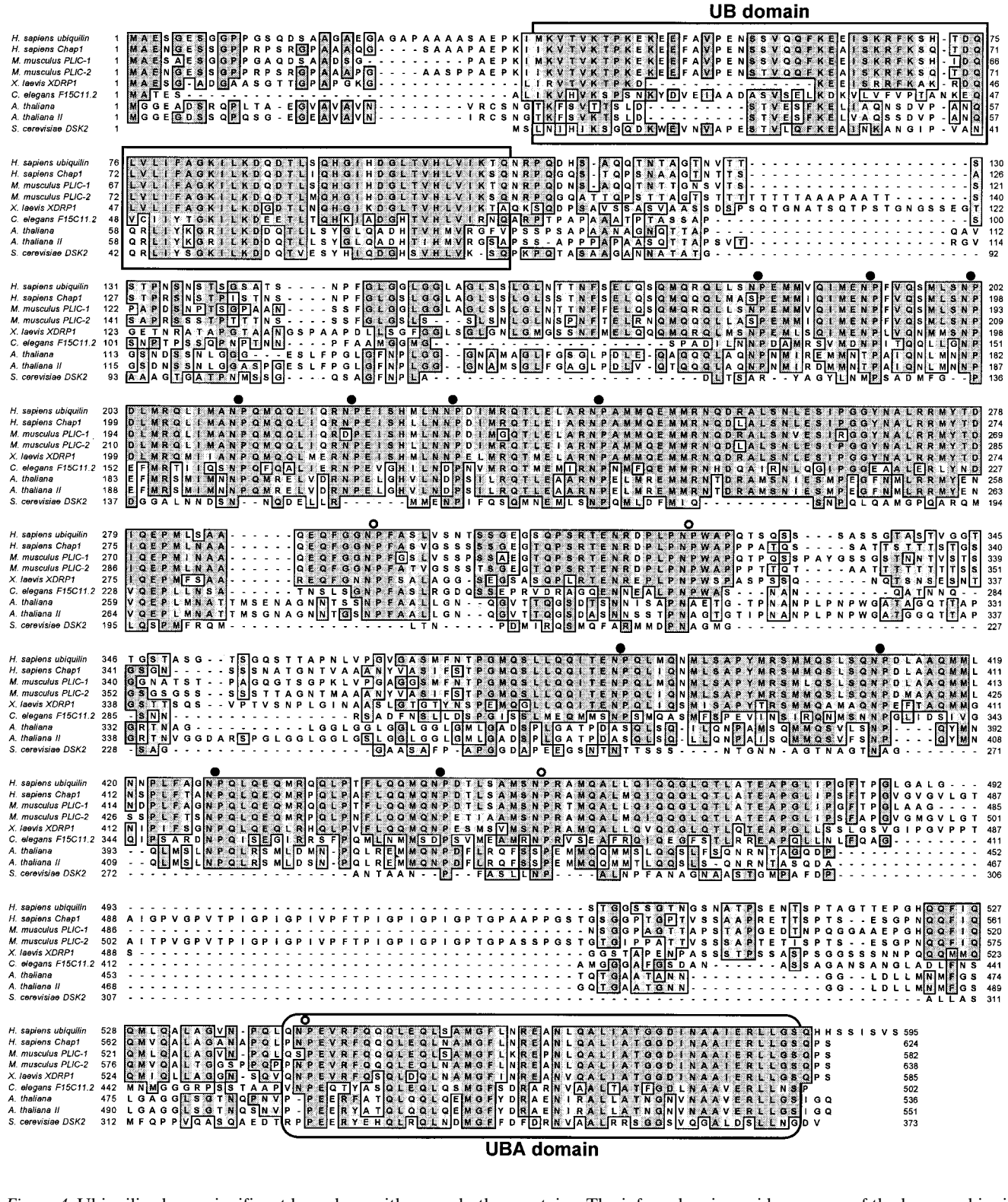

Figure 4. Ubiquilin shares significant homology with several other proteins. The inferred amino acid sequence of the human ubiquilin ORF and its homology to several related proteins: *Homo sapiens* Chap1, a protein involved in binding Hsp70-like Stch protein; *Mus musculus* PLIC-1 and PLIC-2, proteins involved in linking integrins to vimentin; *X. laevis* XDRP1, a protein which binds cyclin A; *C. elegans* F15C11.2 and two *A. thaliana* proteins, proteins with unknown functions; and *S. cerevisiae* DSK2, involved in spindle pole body duplication. Identical residues are darkly shaded, whereas similar residues are lightly shaded. Only homology in five or more sequences are shown. All the proteins contain UB domains (square box) and UBA domains (rounded box), which are extremely well conserved in sequence. In addition, the central region between the UB and UBA domains contain several asparagine-proline repeats, which are either regularly spaced apart (closed circles) or located elsewhere throughout the protein (open circles). The high overall homology of the proteins suggests that they belong to the same multigene family.

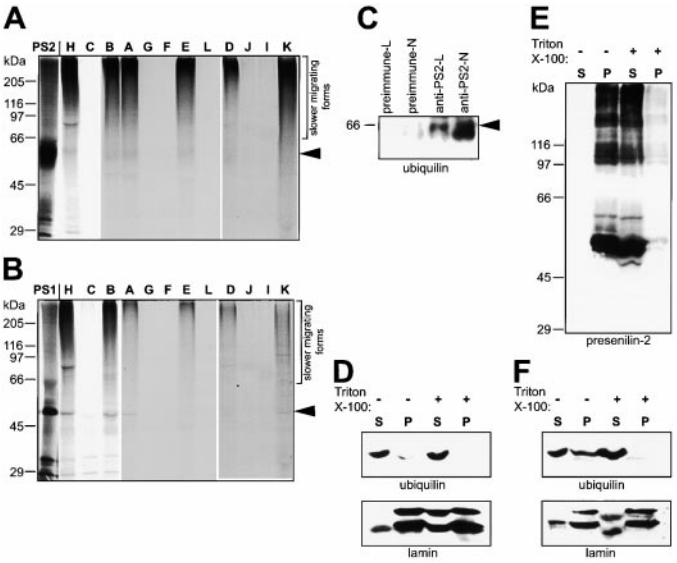

Figure 5. Ubiquilin binds presenilins in vitro. (A and B) GST pull-down experiments. Full-length in vitro synthesized ^{35}S-labeled PS2 and PS1 (first lanes) migrated in SDS-PAGE gels with broad bands of 54 and 48 kD (arrowheads), respectively, along with a smear of slower migrating forms, presumably due to the highly hydrophobic nature of the proteins. [^{35}S]PS complexes (especially the slower migrating forms) were retained by GST–ubiquilin constructs containing the UBA domain (lane letters correspond to constructs shown in Fig. 2 III), but not by those lacking the domain, or by GST alone. (C) Immunoprecipitation experiments. PS2-transfected HeLa cell lysates were immunoprecipitated with preimmune sera or corresponding anti–PS2-Loop antibody and anti-PS2 NH_2 terminus antibody. After separation by SDS-PAGE, coprecipitating ubiquilin (arrowhead) was detected by immunoblotting with anti–ubiquilin-B antibody. (D–F) Cell fractionation experiments. Parallel immunoblots of equal portions of soluble supernatant (S) and insoluble pellet (P) HeLa cellular fractions prepared without the use of detergent (−) or in the presence of 1% Triton X-100 (+) with (D and F) anti-ubiquilin or (E) anti-PS2 antibodies. The HeLa cells used for cell fractionation in D were untransfected, whereas, in E and F, the cells were transfected with a full-length wild-type PS2 construct. The relative ratio of ubiquilin protein in the P− compared with the S− fractions was determined by densitometric analysis of the autoradiographs. This analysis indicated that transfection of presenilin caused 30% more (F) ubiquilin protein to partition in the pellet fraction in the absence of detergent compared with (D) untransfected cells. The partitioning of lamin A/C proteins after cell fractionation from untransfected and PS2-transfected cells was monitored with anti-lamin A/C antibodies and shown below in D and F, respectively.

transcripts (Fig. 2 II, X; Fig. 3 A). Comparison of ubiquilin band intensities after correction for mRNA loading (β-actin control bands) and normalized to the skeletal muscle value suggested that expression of the 4.4-kb transcript was highest in brain and pancreas (Fig. 3 C). Additional Northern blot analysis of mRNA from different subregions of the human brain revealed slight variation (1.0–1.5-fold) of ubiquilin expression with the same 4.4-kb transcript as the predominant species (Fig. 2 II, Y; Fig. 3, B and C).

We determined the chromosomal location of the ubiquilin gene using PCR radiation hybrid mapping (see Materials and Methods; data not shown). This procedure resulted in an unambiguous assignment of ubiquilin nearby to two loci, CHLC.GATA22H04 and CHLC.GATA81C04, located on chromosome 9q22 close to the 9q21.3 border. Interestingly, the chromosome region to which ubiquilin maps is thought to contain a susceptibility gene(s) involved in late-onset AD (Kehoe et al., 1999).

Ubiquilin Contains Ubiquitin-related Protein Domains and Is a Member of a Highly Conserved Gene Family

The complete ubiquilin ORF consists of 595 residues, with a sequence rich in glutamines and serines, 10.9% and 11.1%, respectively, but lacking any cysteines (Fig. 4). The protein has a calculated isoelectric point (pI) of 4.97 and is predicted to be soluble, based on having a high hydrophilic profile using MacVector 6.5 software (Oxford Molecular Group; data not shown). Currently known protein structural motifs residing within ubiquilin include an NH_2-terminal UB domain and a COOH-terminal ubiquitin-associated (UBA) domain, both of which have been implicated in targeting and degradation of proteins by the ubiquitin-proteasome pathway. The predicted ubiquilin protein also contains numerous regularly spaced asparagine-proline (Asn-Pro) repeats of unknown function (Fig. 4). When first sequenced, no apparent mammalian homologue for ubiquilin had been deposited in GenBank/EMBL/DDBJ databases. However, there was significant homology to several full-length genes of unknown function: the *C. elegans* F15C11.2 gene (36% identical) and two related genes in *Arabidopsis thaliana* (34 and 35% identical). In addition, the protein had weak homology to the *Saccharomyces cerevisiae* DSK2 gene (31% identical), which can suppress a KAR1 defect (Biggins et al., 1996). KAR1 is an essential gene involved in the duplication of the yeast microtubule organizing center known as the spindle pole body. Interestingly, ubiquilin homology to DSK2 was primarily confined to the UB and UBA domains. However, since both UB and UBA domains are present in many other proteins, it is uncertain whether ubiquilin and DSK2 are true orthologs.

At about the time the ubiquilin sequence was deposited in GenBank/EMBL/DDBJ, a *Xenopus laevis* protein involved in inhibiting cyclin A–protein degradation, called XDRP1, and having 60% identity to ubiquilin had just been submitted (Funakoshi et al., 1999). Since then, two *Mus musculus* proteins that are thought to interlink integrin-associated proteins with the vimentin cytoskeleton, called PLIC-1 and PLIC-2 (84 and 69% identical, respectively) (Wu et al., 1999), and human Chap1 protein (renamed ubiquilin 2; 79% identical), which binds Hsp70-like Stch and can complement a DSK2 yeast mutant (Kaye et al., 2000), have been described. The high degree of homology among these protein sequences can be seen when aligned by the MacVector 6.5 ClustalW protein alignment program (Fig. 4). This comparison revealed that the human, mouse, and *Xenopus* sequences are more closely related to one another than the *C. elegans*, *A. thaliana*, and *S. cerevisiae* sequences, as would be expected for higher eukaryotes. The former group of proteins all shared extensive homology across the entire length of the ubiquilin polypeptide. The four regions of highest homology include the UB and UBA domains and

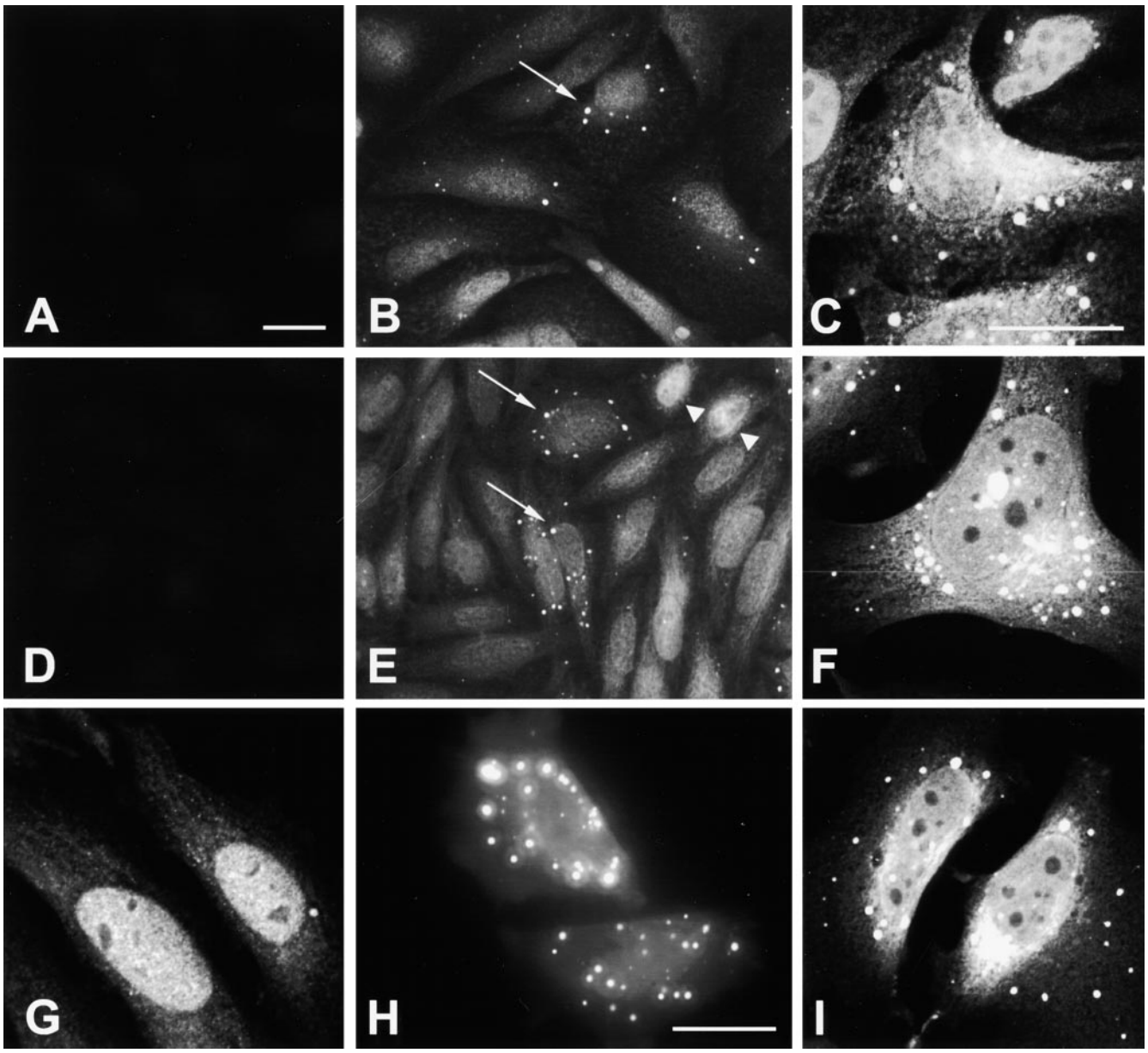

Figure 6. Ubiquilin localizes to the nucleus and cytoplasm. (A, B, D, and E) Indirect immunofluorescence microscopy of endogenous ubiquilin staining in untransfected HeLa cells and (C and F) confocal microscopy of HeLa cells transfected with ubiquilin or (I) myc-tagged ubiquilin. (A and B) Preimmune and the corresponding anti–ubiquilin-B antibody staining, respectively, are shown. (C) Overexpressed ubiquilin as detected with anti–ubiquilin-B antibody. (D and E) Preimmune and the corresponding anti–ubiquilin-C antibody staining, respectively, are shown. (F) Overexpressed ubiquilin is shown, as detected with affinity-purified anti–ubiquilin-C antibody. Both anti-ubiquilin sera showed specific staining in the cytoplasm and nucleus, along with cytoplasmic punctate structures in a subset of the untransfected cells (arrows). The expression levels of ubiquilin protein within the nucleus varied with some cells containing substantially more nuclear protein (arrowheads). Transient overexpression of wild-type ubiquilin caused frequent accumulation of ubiquilin to the intracellular punctate structures. (G) Endogenous ubiquilin is shown, as detected by affinity-purified anti–ubiquilin-C antibody (confocal microscopy). (H) Overexpressed GFP-tagged ubiquilin of live HeLa cells, as seen by fluorescence microscopy, revealed accumulation of the fusion protein to the cytoplasm and to similar punctate structures. (I) Additional evidence for intracellular localization of ubiquilin, using a myc-tagged construct and stained with an anti-myc mAb (confocal microscopy), is shown. Bar, 25 μm.

two stretches rich in Asn-Pro repeats (residues G157–P326 and P375–P482) located between the two ubiquitin-related domains. Differences in the divergent regions are instructive, especially the insert between residues L485–T527 in Chap1, which is conserved in PLIC-2 but missing in ubiquilin, PLIC-1, and XDRP1. Based on the homology between human and mouse sequences, it appears that ubiquilin is more closely related to PLIC-1, whereas Chap1 is more closely related to PLIC-2. Collectively, the proteins are likely to be members of a related multigene family, since at least two independent genes are known to exist in humans, mice, and *A. thaliana*.

Evidence That Ubiquilin Protein Directly Binds PS1 and PS2

GST-fusion proteins containing the UBA domain and nine COOH-terminal residues (QHHSSISVS) of ubiquilin were necessary and sufficient to bind [^{35}S]methionine-radiolabeled PS2 and PS1 in a GST pull-down assay (Fig. 5, A and B, respectively). Interestingly, slower migrating forms of both presenilins were much more tightly bound than the full-length forms. Whether the slower migrating forms are more ubiquitinated, extensively modified, or merely hydrophobic aggregates is not known. As expected, GST alone (Fig. 5, A and B, lane L) did not bind either presenilin. No other region of ubiquilin tested was able to pull-down either of the presenilins, indicating that binding of presenilin to ubiquilin is mediated by sequences spanning the UBA domain and the COOH-terminal tail. These in vitro binding assay results were consistent with the interaction data of ubiquilin recovered in the Y2H screen.

To support the in vitro binding data, coimmunoprecipitation and cell fractionation experiments between PS2 and endogenous ubiquilin were also performed. PS2-transfected HeLa cell extracts were immunoprecipitated with two different anti-PS2 specific antibodies, separated by SDS-PAGE, and immunoblotted with anti–ubiquilin-B antibodies. Ubiquilin protein coimmunoprecipitated with both of the anti-PS2 antibodies, one raised against the loop and the other to the NH_2-terminal sequences, but did not coimmunoprecipitate when the preimmune sera was used (Fig. 5 C). Additional verification of ubiquilin binding to PS2 was obtained in cell fractionation studies. Untransfected and PS2-transfected HeLa cells were fractionated either in the absence or presence of Triton X-100 detergent into soluble and insoluble fractions. Equivalent amounts of the fractions were then immunoblotted to determine the amount of ubiquilin protein in the two fractions. In untransfected cells, almost all of the ubiquilin protein was present in the soluble fraction, independent of detergent treatment (Fig. 5 D, lanes S− and S+). This is consistent with the predicted hydrophilic nature of ubiquilin protein. However, in PS2-transfected cells, 30% more ubiquilin protein separated with the pellet fraction in the absence of detergent treatment (Fig. 5 F, lane P). This change in solubility is likely a consequence of ubiquilin binding to overexpressed membrane-bound PS2, which also fractionated in the insoluble membrane-containing pellet fraction (Fig. 5 E, lane P−). As expected for integral membrane proteins, Triton X-100 treatment caused the release of PS2 into the soluble fraction (Fig. 5 E, lane S+), which coincided with ubiquilin once again separating completely in the soluble fraction (Fig. 5 F, lane S+).

Ubiquilin Localizes To the Nucleus and Cytoplasm

To determine the intracellular distribution of ubiquilin we used rabbit pAb that we had generated to two different GST–ubiquilin fusion proteins (see Materials and Methods). Both antisera detected endogenous and overexpressed 66-kD ubiquilin polypeptides, which were not detected by the preimmune sera (Fig. 3 D). Although one antiserum reacted with an unknown protein of ~55 kD (Fig. 3 E), this reactivity was subsequently removed by affinity purification of the antibody (Fig. 3 F). Immunofluorescence staining of ubiquilin within cells was performed with the specific anti-ubiquilin antibodies. Compared with the preimmune sera (Fig. 6, A and D), both antibodies revealed similar staining patterns (Fig. 6, B and E). Indirect immunofluorescence, as well as laser confocal microscopy, revealed endogenous intracellular localization of ubiquilin in HeLa cells to both the nucleus and cytoplasm (Fig. 6, B, E, and G). In some cells, endogenous ubiquilin staining was stronger in the nucleus (Fig. 6 E, arrowheads). Furthermore, in a small subset of cells, ubiquilin within the cytoplasm was localized to punctate structures (Fig. 6, B and E, arrows). The frequency of these structures dramatically increased upon overexpression of full-length untagged ubiquilin (Fig. 6, C and F). To corroborate the anti-ubiquilin staining pattern, we performed additional localization studies on myc- and GFP-tagged ubiquilin proteins in HeLa cells (Fig. 2 IV, O and N, respectively). Overexpressed myc-tagged ubiquilin stained with anti-myc mAb exhibited the same intracellular structures (Fig. 6 I) as overexpressed wild-type ubiquilin (Fig. 6, C and F). Finally, the same fluorescent staining pattern was reproduced upon overexpression of GFP-ubiquilin (Fig. 6 H). Since the GFP-ubiquilin image in Fig. 6 H was captured from live and unfixed cells without antibodies, this established that the anti-ubiquilin structures seen previously were not artifacts of the paraformaldehyde fixation or immunofluorescence staining procedures.

Intracellular Colocalization of the Presenilin and Ubiquilin Proteins

As overexpressed presenilin proteins are localized predominantly to the ER, and ubiquilin protein in HeLa cells is found throughout the nucleus and cytoplasm, we determined if ubiquilin colocalized with the presenilins when the latter were overexpressed. Indeed, there was a dramatic change in ubiquilin staining in HeLa cells coexpressing either PS1 or PS2 and ubiquilin, resulting in almost complete colocalization of the presenilin and ubiquilin intracellular staining patterns, as seen by laser confocal immunofluorescence microscopy (Fig. 7, A and B). Careful examination of the colocalized proteins revealed ubiquilin staining to be punctate, whereas presenilin staining could be traced to an ER-like pattern. Particularly striking was colocalization of ubiquilin with irregularly shaped presenilin-enriched structures within the cytoplasm of overexpressing cells. In contrast, there was little colocalization in the nucleus where ubiquilin, but not presenilin, staining could be found.

Since Y2H data suggested that ubiquilin interacts with both the loop and COOH-terminal domains of the presenilins, we examined whether removal of these regions from PS2 would abolish colocalization of the proteins in vivo. To assess this possibility, two PS2 constructs containing progressively longer COOH-terminal deletions were made. In the first, PS2(ΔC), the 39-amino acid COOH-terminal domain was deleted (Fig. 1 A, arrowhead), whereas in the second, PS2(ΔLC), the large hydrophilic loop and all sequences downstream were deleted (Fig. 1 A, arrow). When expressed in HeLa cells, PS2(ΔC) still colocalized with ubiquilin (Fig. 7 C), presumably since the PS2 loop region that remained could bind ubiquilin, as suggested by the strong interaction between the two in Y2H assays (Fig. 1 D). However, once

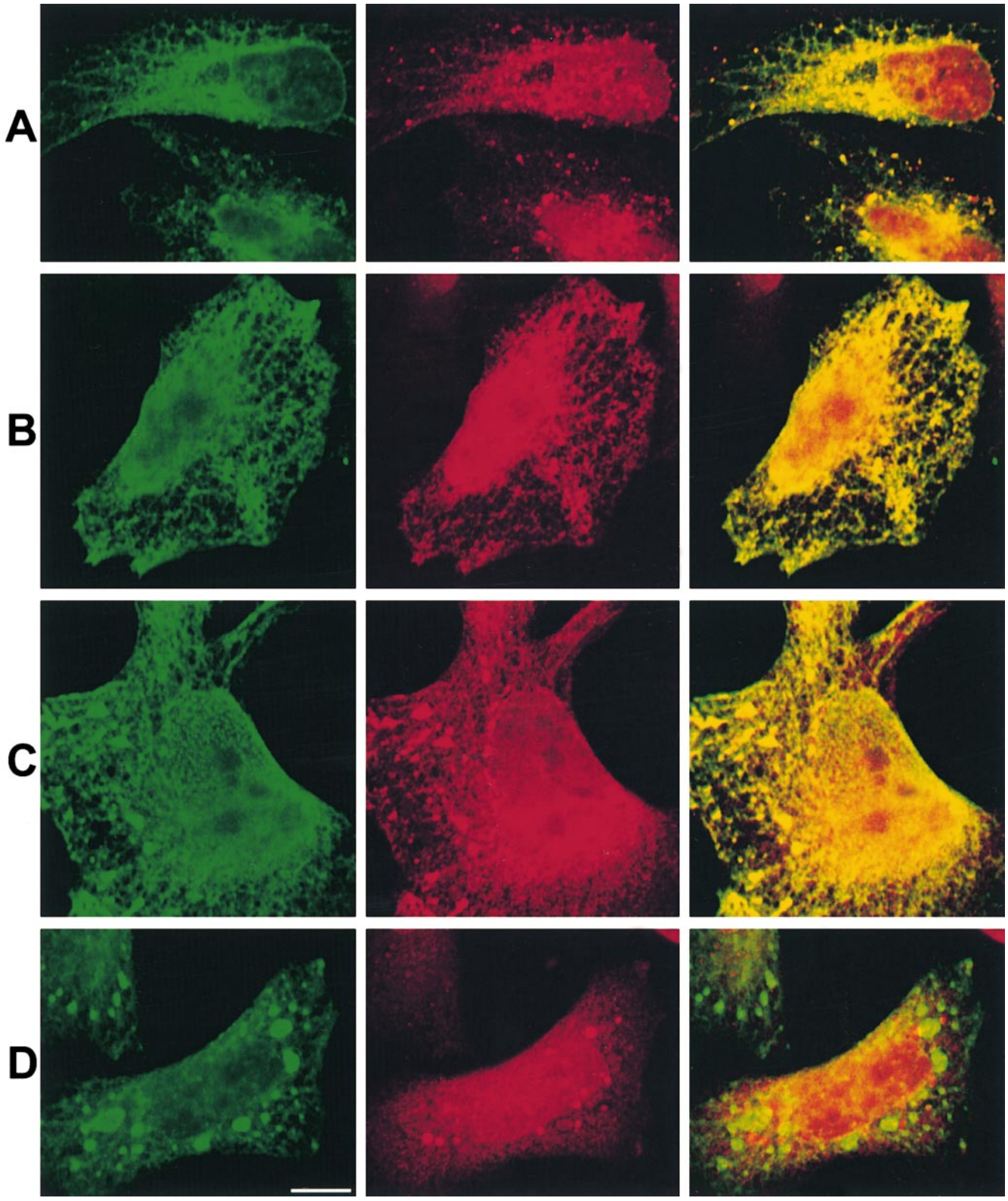

Figure 7. Intracellular colocalization between ubiquilin and the presenilins. (A–D) HeLa cells were cotransfected with ubiquilin and either (A) wild-type PS1, (B) wild-type PS2, (C) PS2(ΔC) deletion mutant, or (D) PS2(ΔLC) deletion mutant and costained with appropriate goat anti-presenilin antibodies (left images) and affinity-purified rabbit anti–ubiquilin-C antibody (center images). The green (fluorescein) and red (rhodamine) confocal images in each row were merged and shown on the right, with yellow indicating colocalization of ubiquilin and presenilin proteins. Bar, 10 μm.

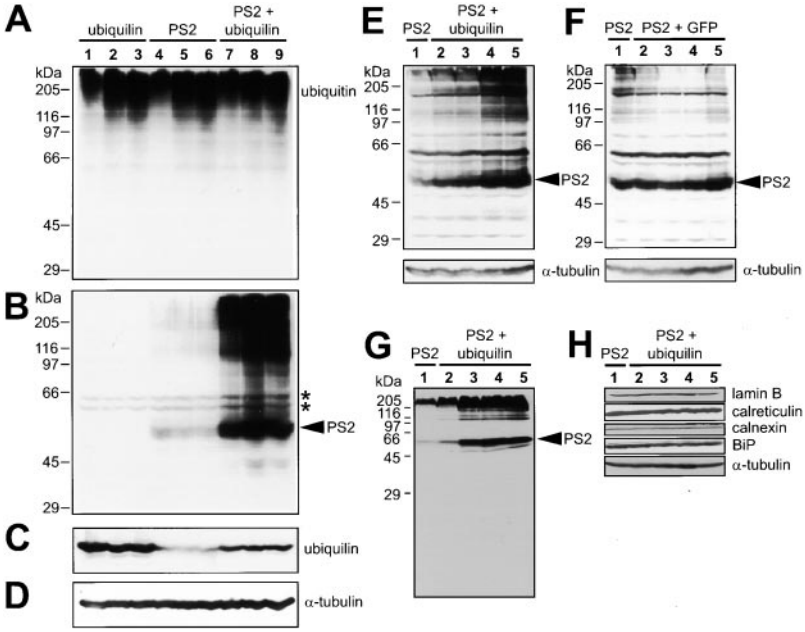

Figure 8. Ubiquilin promotes increased PS2 protein accumulation. (A–D) HeLa cells, 12 h after transfection with ubiquilin (15 μg expression plasmid, lanes 1–3), PS2 (7 μg expression plasmid, lanes 4–6), or both (lanes 7–9), were either left untreated (lanes 1, 4, and 7) or treated for 5–6 h with proteasome inhibitors (20 μM synthetic lactacystin in lanes 2, 5, and 8; 40 μM MG-132 in lanes 3, 6, and 9). Equivalent amounts of protein (100 μg) from each sample were immunoblotted with (A) anti-ubiquitin, (B) anti-PS2-NH_2 terminus, (C) affinity-purified anti–ubiquilin-C, or (D) anti-α-tubulin antibodies. As expected, anti-ubiquitin antibodies detected larger molecular weight proteins in cells treated with proteasome inhibitors (lanes 2 and 3, 5 and 6, and 8 and 9) compared with untreated cells (lanes 1, 4, and 7). Significantly more PS2 protein (and slower migrating forms) could be seen in cells cotransfected with ubiquilin (lanes 7–9, arrowhead) compared with those transfected with PS2 alone (lanes 4–6). (*) A doublet of weakly reactive bands was detected in all lysates, but we considered them to be nonspecific proteins. The anti–α-tubulin blot shows equal protein loading of each sample. (E) HeLa cells were transfected with PS2 alone (9 μg expression plasmid, lane 1) or cotransfected along with increasing amounts of ubiquilin (1, 2, 3, or 4 μg expression plasmid in lanes 2–5, respectively). Equivalent amounts of the transfected lysates were separated through an 8.5% polyacrylamide gel and immunoblotted with anti–PS2-NH_2 terminus antibody. (F) Same as in E, except with the same increasing amounts of GFP expression plasmid (lanes 2–5) instead of ubiquilin. (G) Same as in E, but proteins were separated on a 10% polyacrylamide gel and immunoblotted with anti–PS2-loop antibody. Note the absence of any detectable PS2 cleavage products corresponding to endoproteolytic PS2 cleavage in the loop. (H) The same blot shown in G or parallel blots were immunoblotted for lamin B, calreticulin, calnexin, BiP, and α-tubulin. The relative levels of these other endogenous proteins remained relatively unchanged compared with the PS2 levels.

the hydrophilic loop region and COOH terminus were both removed, PS2(ΔLC) no longer colocalized with ubiquilin (Fig. 7 D), suggesting that the NH_2 terminus and the first six transmembrane domains of PS2 do not contain additional ubiquilin binding sites. A notable feature of the overexpression of PS2(ΔLC) was its accumulation into large spherical aggregates that failed to stain positively for ubiquilin.

Ubiquilin Expression Promotes Increased Accumulation of Presenilin Proteins

Since ubiquilin contains multiple ubiquitin-related structural motifs, we investigated whether its association with presenilin would have an effect on presenilin-protein modification and/or stability. Treatment of mock-transfected and PS2-transfected HeLa cells with proteasome inhibitors lactacystin (20 μM) or MG-132 (40 μM), as expected, increased the overall amount of ubiquitinated proteins in cells (Fig. 8 A, lanes 2 and 3, 5 and 6, and 8 and 9 versus lanes 1, 4, and 7, respectively). However, these conditions did not markedly increase PS2 protein levels (Fig. 8 B, lanes 4–6). Remarkably, coexpression of ubiquilin with PS2 caused a substantial (>10-fold) increase in PS2 protein accumulation (Fig. 8 B, lanes 7–9) compared with overexpression of PS2 alone (Fig. 8 B, lanes 4–6). This effect was independent of treatment with lactacystin or MG-132, as it also occurred just as robustly in cells not treated with the proteasome inhibitors. Particularly striking was the increased accumulation in SDS-PAGE gels of full-length uncleaved PS2 protein (Fig. 8 B, arrowhead) and higher molecular weight complexes that PS2 forms. Increasing the amount of transfected ubiquilin plasmid DNA, whereas maintaining constant levels of transfected PS2 plasmid DNA, revealed a dose-dependent effect by ubiquilin on PS2 accumulation within the cells (Fig. 8 E, lanes 1–5). This effect was specific for ubiquilin expression, since cotransfection of increasing amounts of GFP plasmid DNA with PS2 did not increase PS2 protein accumulation (Fig. 8 F, lanes 1–5). The blot in Fig. 8 E was exposed for a shorter time than that in Fig. 8 F to optimally illustrate the subtle changes in PS2 protein levels. In these experiments, we routinely observed the accumulation of full-length PS2 protein, but not the endoproteolytic cleaved forms of the protein (Haass and De Strooper, 1999). In fact, recent reports have indicated that cleavage of presenilins is not essential for biological function of the presenilins, namely by its ability to rescue PS activity in *C. elegans* (Jacobsen et al., 1999; Steiner et al., 1999). The absence of detectable endoproteolytic cleaved forms of PS2 is more clearly illustrated in Fig. 8 G, which shows that an antibody specific for PS2-loop sequences downstream of the proposed endoproteolytic cleavage site recognized the same 54 kD and higher PS2 species (as the PS2 NH_2-terminal specific antibody). Interestingly, though ubiquilin caused a dose-dependent increase in presenilin accumulation, it did not alter the accumulation levels of various other endogenous HeLa proteins, such as lamin B, calreticulin, calnexin, BiP, and α-tubulin (Fig. 8 H). Similar experiments repeated with PS1 indicated that ubiquilin also promoted a dose-dependent increase in PS1 protein accumulation in HeLa cells (data not shown).

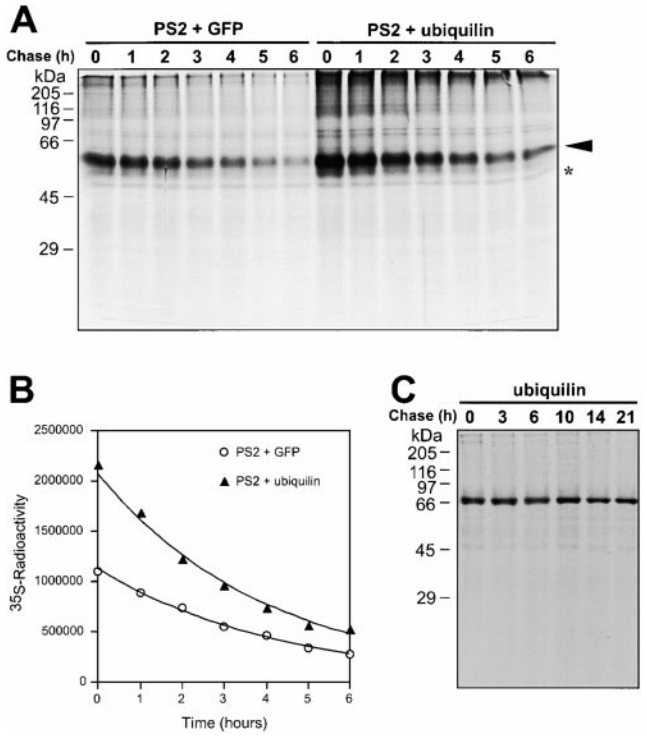

Figure 9. Ubiquilin facilitates increased presenilin protein expression but does not substantially change presenilin protein turnover. (A) HeLa cells, electroporated with a mixture of either PS2 and GFP expression plasmids (7 μg PS2 and 15 μg pEGFP-C1) or with PS2 and ubiquilin expression plasmids (7 μg PS2 and 15 μg ubiquilin), were pulse labeled with [^{35}S]methionine for 1 h and then chased with nonradioactive medium for 0–6 h. At appropriate time intervals (indicated above each lane), the cells were lysed and PS2 protein was immunoprecipitated using a rabbit anti–PS2-loop antibody. The immunoprecipitated proteins were separated by SDS-PAGE through an 8.5% gel, and the radioactivity of the band corresponding to full-length PS2 (arrowhead) in each lane was determined by phosphoimage analysis. (*) The light band was probably a nonPS2 related protein whose radioactivity changed little during the chase period of the experiment and was therefore useful for normalizing protein amounts loaded in each lane. (B) Graph showing an exponential decline of pulse-labeled PS2 protein over time. The calculated half-life of PS2 in this experiment was ~3.1 and 2.9 h when coexpressed with GFP or ubiquilin, respectively. In this and in two other experiments, ~1.4–1.6-fold more PS2 protein was synthesized (after normalization) when coexpressed with ubiquilin than with GFP. (C) Mock-electroporated HeLa cells were pulse labeled with [^{35}S]methionine for 1 h and then chased with nonradioactive medium for 0–21 h. Ubiquilin protein was immunoprecipitated from the lysates using rabbit anti–ubiquilin-C antibodies. The radioactivity of the immunoprecipitated ubiquilin band was determined by phosphoimage analysis. This analysis revealed a small decline in radioactivity (15% reduction) over 21 h, indicating that the endogenous ubiquilin in HeLa cells is long-lived, with an estimated half-life of ~90 h.

Ubiquilin Facilitates Increased PS2 Expression but Does Not Dramatically Alter PS2 Protein Turnover

To determine if the ubiquilin-induced increase in presenilin accumulation is due to a change in the rate of presenilin protein turnover, we carried out pulse-chase experiments of HeLa cells in which PS2 protein was coexpressed with either ubiquilin or GFP (as a control). PS2 protein in the pulse-chase lysates was immunoprecipitated using an anti–PS2-loop antibody and resolved by SDS-PAGE (Fig. 9 A). Phosphoimage analysis of the immunoprecipitated full-length PS2 band (~54 kD), indicated that the half-life of PS2 protein to be approximately similar. 3.1 and 2.9 h when coexpressed with GFP or ubiquilin, respectively (Fig. 9, A and B). Apart from the prominent PS2 band at 54 kD, a smear of bands with varying intensity was resolved after SDS-PAGE, using the PS2-loop antibody for immunoprecipitation. Some of these bands appear to be PS2 related, especially the higher molecular weight species, as they corresponded to similar PS2 immunoreactive species using this and other PS2 antibodies (Fig. 8, E and G) (Janicki and Monteiro, 1997, 1999). Phosphoimage analysis of the smear of bands above the 97-kD marker indicated that the rate of turnover of these larger PS2 complexes was also similar in both GFP- and ubiquilin-coexpressing cells (data not shown).

A notable difference of these pulse-labeling experiments was the increased amount of immunoprecipitated PS2-labeled proteins in cells that were overexpressing ubiquilin, compared with GFP. Despite using similar amounts of PS2 DNA for electroporation within parallel-labeling experiments, we routinely obtained a 1.6–2.0-fold increase in PS2-labeled protein when PS2 was coexpressed with ubiquilin compared with GFP. This effect was seen in three separate experiments (data not shown). Overall, these results suggest that the ubiquilin-induced elevation in presenilin accumulation does not involve a substantial change in the rate of presenilin–protein turnover, but instead may facilitate increased PS2 protein synthesis. Finally, to determine the rate of endogenous ubiquilin protein turnover, we performed another pulse-chase experiment of mock-transfected HeLa cells and immunoprecipitated the endogenous ubiquilin protein using our anti–ubiquilin-C antibody (Fig. 9 C). Phosphoimage analysis indicated that pulse labeled ubiquilin decays exceedingly slowly, only 15% over the 21 h chase period, from which we estimate the half-life of the protein to be 90 h.

Immunohistochemistry of Human Brain Tissue Sections Reveals Ubiquilin Immunoreactivity in Neurons As Well As within Neuropathological Lesions Such As Neurofibrillary Tangles and Lewy Bodies

Since neuropathological lesions in AD and PD have been found to be highly immunoreactive to ubiquitin antibodies, we investigated whether these structures may also contain ubiquilin immunoreactivity. Immunohistochemistry of adult human brain sections was performed with anti–ubiquilin-B and anti–ubiquilin-C antibodies. The former was raised against ubiquilin polypeptides that were devoid of the UB domain, whereas the latter was raised against ubiquilin polypeptides lacking the UBA domain as well (Fig. 2 III, B and C, respectively). Compared with the preimmune sera, which showed no specific staining (Fig. 10, A and C), both antibodies strongly stained neurons with little, if any, staining of glia (Fig. 10, B, D, and E). In general, the anti–ubiquilin-C antibody stained neurons with greater clarity and intensity. As with cultured cells, anti-ubiquilin staining in neurons was to the nucleus and the cytoplasm. In addition, there is clear evidence for ubiquilin staining within long axonal processes (Fig. 10 D). Interestingly, neurons containing neurofibrillary tangles (NFTs) from AD affected brains seemed to stain more intensely compared with control neurons (Fig. 10 E and F). Moreover, examination of ubiquilin staining in brains afflicted with PD (not shown) and diffuse LB disease revealed robust staining of Lewy bodies (Fig. 10 H).

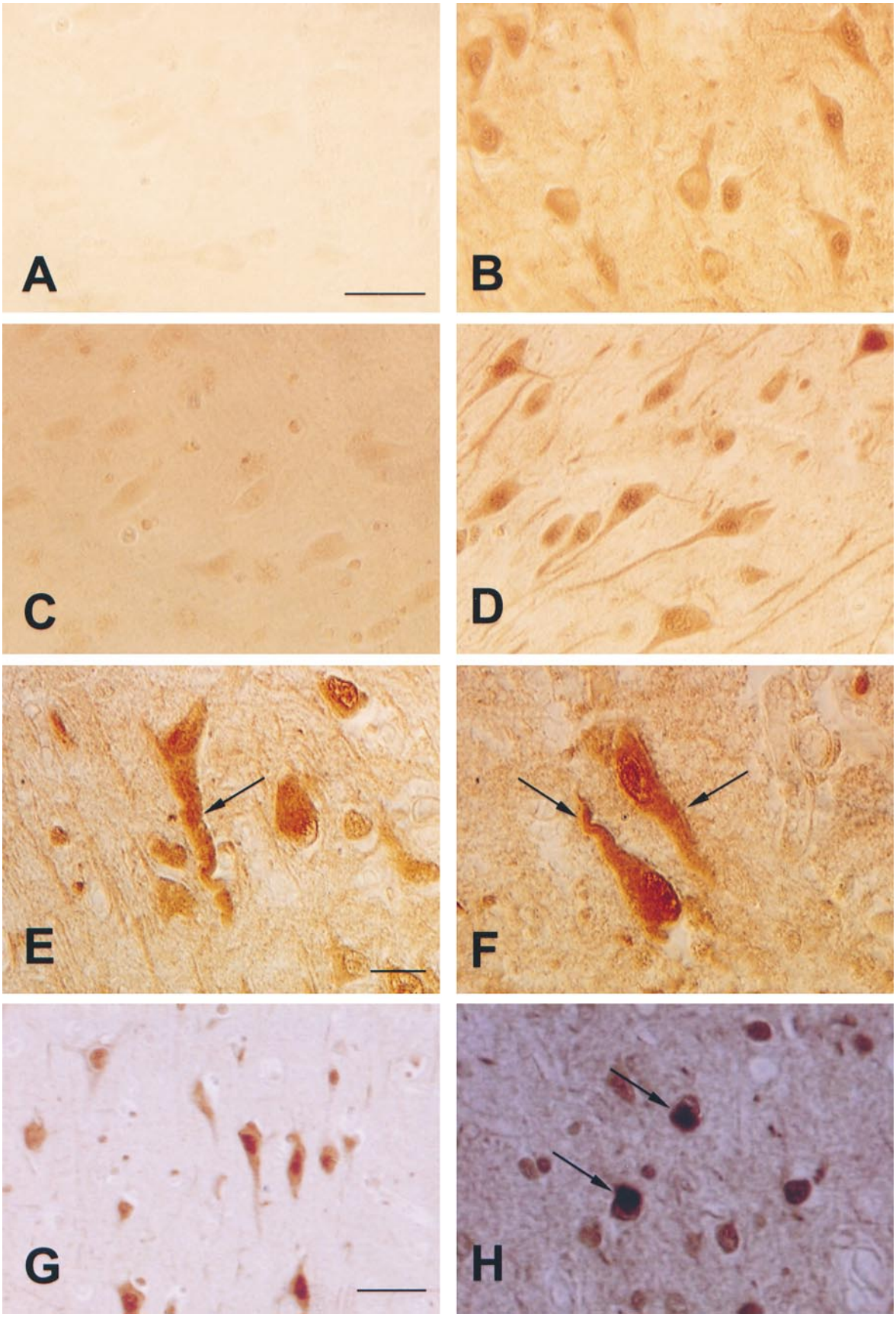

Figure 10. Anti-ubiquilin staining of human brain tissue reveals strong staining of neurons in human brain and robust staining of NFTs and Lewy bodies of AD and PD, respectively. Sections of human brain were stained with either the preimmune or anti–ubiquilin-B and anti–ubiquilin-C antibodies. (A–D) Consecutive sections of the hippocampus of an AD afflicted brain were stained with either the (A and C) preimmune serum or with their corresponding (B) anti–ubiquilin-B and (D) anti–ubiquilin-C antibodies. (E and F) Examples of strong staining of NFTs (arrows) in hippocampal sections of AD afflicted brains with anti–ubiquilin-C antibodies. (G) Anti–ubiquilin-C antibody staining of a control nonAD human brain showing strong staining of neurons. (H) Cortical human brain section of a DLBD afflicted brain showing strong anti–ubiquilin-C staining of Lewy bodies (arrows). Bars: (A–D and G and H) 40 μm; (E and F) 20 μm.

Discussion

Here, we describe a novel human presenilin-interacting protein named ubiquilin. Y2H interaction, GST pull-down experiments, coimmunoprecipitation studies, changes in the cellular fractionation of proteins, and colocalization of the proteins expressed in vivo provide compelling evidence that ubiquilin and the presenilins interact with one another. Ubiquilin is an important protein because it contains multiple ubiquitin-related domains typically thought to be involved in targeting proteins for degradation, yet ubiquilin promotes increased presenilin protein accumulation. Moreover, ubiquilin is highly expressed in neurons of human brain and is associated with NFTs and Lewy bodies of AD and PD brains, respectively.

The promotion of presenilin protein accumulation by ubiquilin overexpression is noteworthy as a new means by which presenilin levels may be modulated. By conducting pulse-chase experiments, we found that ubiquilin induced an increase in presenilin protein maturation, but did not dramatically affect presenilin protein turnover. The net effect over time from increased presenilin protein synthesis and undisturbed turnover rate would eventually lead to an elevation of the intracellular pool of presenilin proteins. This modulation of presenilin levels by ubiquilin may have important consequences to cellular functions, as presenilins have been linked to various biological processes, including Notch signaling, calcium regulation, apoptosis, cell cycle regulation, unfolded-protein response, as well as APP-associated gamma secretase activity (see Introduction).

It will be interesting to determine the precise mechanism by which ubiquilin induces increased presenilin protein synthesis. Ubiquilin could increase presenilin synthesis by simply increasing presenilin transcription, increasing presenilin translation, or facilitating correct polypeptide folding, maturation, and intracellular targeting of the polytopic transmembrane presenilin protein. Based on its various properties, we are especially intrigued by the possibility that ubiquilin may act as a molecular chaperone. (a) Studies of the *Xenopus* ubiquilin homologue, XDRP1, have suggested that ubiquilin can act posttranscriptionally like a molecular chaperone and prevent degradation of in vitro translated cyclin A protein (Funakoshi et al., 1999). (b) Chap1 (ubiquilin 2) has been shown to bind Stch, an Hsp70-like protein (Kaye et al., 2000). In turn, many heat-shock proteins have been shown to function as molecular chaperones, preventing protein aggregation and protein degradation (Warrick et al., 1999; Krobitsch and Lindquist, 2000). (c) Recent evidence has linked ubiquilin proteins to the proteasome (Kleijnen et al., 2000). Meanwhile, the 19S regulatory subunit of the 26S proteasome (the degradation complex for ubiquitin-tagged proteins) has been shown to possess protein-unfolding activity (Braun et al., 1999). (d) Indirect evidence that ubiquilin may aid in presenilin protein folding or targeting comes from our observation that the presenilin construct PS2(ΔLC), with deletions of both the loop and COOH-terminal ubiquilin-interaction sites (as demonstrated by Y2H assays and lack of colocalization with ubiquilin within cells), frequently accumulated into large cytoplasmic aggregates. In contrast, presenilin molecules, which contained ubiquilin interaction sites, rarely formed large protein aggregates. The connection between aggregate accumulation and loss of ubiquilin interaction may be entirely coincidental. However, the possibility that the two are interconnected cannot be discounted. Finally, presenilins proteins have themselves been linked to molecular chaperones of the ER, which are involved in the unfolded-protein response (Katayama et al., 1999; Niwa et al., 1999).

Another mechanism by which ubiquilin might increase presenilin accumulation is to alter presenilin degradation rates, especially that of the ubiquitinated forms of presenilins. In fact, a recent report by Kleijnen et al. (2000) found evidence that overexpression of human ubiquilin proteins, hPLIC-1 (ubiquilin 1) and hPLIC-2 (ubiquilin 2), interfered with ubiquitin-dependent degradation of p53 and IkBα. Although we did not find any significant change in the turnover rate of the major 54-kD PS2 polypeptide species (corresponding to full-length PS2), we cannot exclude the possibility that certain ubiquitinated forms of presenilins may have altered turnover rates. The ubiquitinated forms of presenilins migrated as a smear on the SDS-PAGE gels, which made quantification of the turnover rates of these species difficult. It will be important in future studies to determine if ubiquilin is involved in ubiquitin-dependent degradation of presenilins.

The region in ubiquilin that binds presenilins was mapped to the COOH-terminal region containing the UBA domain, which is highly conserved in ubiquilin family members from human to yeast (Fig. 4). This sequence was both necessary and sufficient to bind PS1 and PS2 in vitro. The UBA domain is a recently recognized motif present in one or two copies in a variety of proteins involved in the ubiquitin/proteasome folding/degradation pathway, UV excision repair, and phosphorylation (Hofmann and Bucher, 1996). The UBA domain consists of ~55 total residues of which 45 appear to be core residues. 15 of the core residues are extremely well conserved, suggesting they may be important for determining the overall structure of the domain. Through nuclear magnetic resonance, the structure of the COOH-terminal UBA domain of the human DNA repair protein HHR23A (RAD23 homologue) has been determined. It is a compact three-helix bundle with an exposed hydrophobic surface predicted to be involved in protein–protein interactions (Dieckmann et al., 1998). The strong binding of the ubiquilin UBA domain to presenilins may be facilitated by similar protein–protein interactions. It will be important to determine if sequence variation of the UBA domain in different proteins influences binding specificity to different target proteins.

In vitro binding assays indicated that the UB domain in the NH_2-terminal portion of ubiquilin was not required for binding presenilins. Although this domain shares high homology to the conserved 76-amino acid ubiquitin polypeptide, it is unlikely to be involved in covalent linkage to lysine residues of target proteins, since it lacks the obligate COOH-terminal glycine residue required for cleavage and conjugation. Another possibility could be that the UB domain is modified by conjugation by either ubiquitin or other small ubiquitin-like proteins (e.g., SUMO, NEDD8, etc.) to its lysine group (or groups) forming ubiquitin-conjugates (Pickart, 1998). This is also unlikely to occur, as ubiquilin immunoblots did not show the expected ladder of ubiquitin-conjugated bands. Therefore, the UB domain may play a

role in some other function. For example, in yeast RAD23 and its human homologues (HHR23A and HHR23B), the UB domains are involved in binding subunits of the proteasome, whereas in XDRP1, the UB domain is necessary for binding cyclin A. Clearly, insight into ubiquilin's function will emerge from an understanding of protein–protein interactions and the roles of its different domains.

Using a combination of immunological and GFP-tagging approaches, we have demonstrated that ubiquilin is localized to both the nucleus and the cytoplasm in HeLa cells. The intensity of nuclear staining was variable, with some nuclei staining very brightly. The variability may be related to cell cycle changes of cyclin A (a protein to which ubiquilin's homologue XDRP1 has been shown to interact) levels within the nucleus. The cytoplasmic distribution of ubiquilin was also variable. In untransfected cells, endogenous ubiquilin had a fine punctate appearance, with hints of association to a network-like pattern, possibly the ER. In some of these cells, ubiquilin accumulated in larger spherical structures throughout the cytoplasm, whose number and size were variable. Upon ubiquilin overexpression, the cells formed even larger and more numerous ubiquilin-containing structures. Under confocal microscopy, the ubiquilin staining pattern colocalized almost perfectly with the presenilin staining pattern. Considering that the two presenilin interaction sites (COOH terminus and loop domains) both face the cytoplasm according to the predicted topology of presenilins in membranes, it is not surprising that ubiquilin colocalized with ER membrane-bound presenilin. Still, many other proteins have also been shown to interact with these two domains of presenilins. Clearly, understanding the dynamics of the different protein–protein interactions should provide clues regarding presenilin functions. A study of mouse PLIC-1 and PLIC-2 suggested an involvement in linking integrins via integrin-associated proteins to the vimentin cytoskeleton (Wu et al., 1999). We have not observed any significant staining of ubiquilin to the cell periphery and do not know if this is in any way related to the lack of expression of particular integrin-associated proteins or integrins in HeLa cells. Nevertheless, it is interesting that vimentin and presenilins have been linked to one another in aggresomes, structures involved in the cellular response to misfolded proteins (Johnston et al., 1998). Moreover, recent evidence indicates that aggresomes are involved in the recruitment of the proteasome Hsp70 and chaperones (Garcia-Mata et al., 1999), which circumstantially suggests a mechanism by which ubiquilin could be associated with proteins of the misfolded protein response.

There are the several lines of evidence that link ubiquitin to genes and tissues involved in AD. First, presenilin proteins are thought to be ubiquitinated, since treatment with proteasome inhibitors cause the accumulation of large complexes, which migrate in SDS gels in a manner consistent with modification by ubiquitin (Kim et al., 1997; Fraser et al., 1998; Honda et al., 1999). Second, it is well known that ubiquitin immunoreactivity is strongly associated with the NFTs and senile plaques of AD, hallmark lesions of AD pathology (Mori et al., 1987; Perry et al., 1987). The strong ubiquilin immunoreactivity associated with NFTs and Lewy bodies is intriguing, considering that these lesions are known to contain misfolded proteins. At present, our results do not provide clues as to whether ubiquilin is acting in a causative role or as an end result of association with misfolded and accumulated proteins. We plan to pursue this in the future.

In summary, ubiquilin is the first presenilin-interacting protein, to our knowledge, that has been found to regulate presenilin levels in cells. The presence of multiple ubiquitin-related domains suggests ubiquilin may be involved in the regulation of presenilin protein levels by the proteasome-folding and/or degradation pathway.

We thank Dr. Susan M. Janicki for initiating the Y2H screen, Chung Cho for help with the immunoblots in Fig. 8, G and H, and Dr. Ann F. Pluta and Stacy M. Stabler for critical comments on the manuscript.

This work was funded in part by grants from the National Institute on Aging AG11386 and AG16839 to M.J. Monteiro.

Submitted: 29 February 2000
Revised: 12 September 2000
Accepted: 26 September 2000

References

Biggins, S., I. Ivanovska, and M.D. Rose. 1996. Yeast ubiquitin-like genes are involved in duplication of the microtubule organizing center. *J. Cell Biol.* 133:1331–1346.

Braun, B.C., M. Glickman, R. Kraft, B. Dahlmann, P.M. Kloetzel, D. Finley, and M. Schmidt. 1999. The base of the proteasome regulatory particle exhibits chaperone-like activity. *Nat. Cell Biol.* 1:221–226.

Cotman, C.W. 1998. Apoptosis decision cascades and neuronal degeneration in Alzheimer's disease. *Neurobiol. Aging*. 19:S29–S32.

Davis, J.A., S. Naruse, H. Chen, C. Eckman, S. Younkin, D.L. Price, D.R. Borchelt, S.S. Sisodia, and P.C. Wong. 1998. An Alzheimer's disease-linked PS1 variant rescues the developmental abnormalities of PS1-deficient embryos. *Neuron*. 20:603–609.

Dieckmann, T., E.S. Withers-Ward, M.A. Jarosinski, C.F. Liu, I.S. Chen, and J. Feigon. 1998. Structure of a human DNA repair protein UBA domain that interacts with HIV-1 Vpr. *Nat. Struct. Biol*. 5:1042–1047.

Donoviel, D.B., A.K. Hadjantonakis, M. Ikeda, H. Zheng, P.S. Hyslop, and A. Bernstein. 1999. Mice lacking both presenilin genes exhibit early embryonic patterning defects. *Genes Dev*. 13:2801–2810.

Fraser, P.E., G. Levesque, G. Yu, L.R. Mills, J. Thirlwell, M. Frantseva, S.E. Gandy, M. Seeger, P.L. Carlen, and P. St George-Hyslop. 1998. Presenilin-1 is actively degraded by the 26S proteasome. *Neurobiol. Aging*. 19:S19–S21.

Funakoshi, M., S. Geley, T. Hunt, T. Nishimoto, and H. Kobayashi. 1999. Identification of XDRP1; a *Xenopus* protein related to yeast Dsk2p binds to the N-terminus of cyclin A and inhibits its degradation. *EMBO (Eur. Mol. Biol. Organ.) J*. 18:5009–5018.

Garcia-Mata, R., Z. Bebok, E.J. Sorscher, and E.S. Sztul. 1999. Characterization and dynamics of aggresome formation by a cytosolic GFP-chimera. *J. Cell Biol.* 146:1239–1254.

Georgakopoulos, A., P. Marambaud, S. Efthimiopoulos, J. Shioi, W. Cui, H.C. Li, M. Schutte, R. Gordon, G.R. Holstein, G. Martinelli, P. Mehta, V.L. Friedrich, Jr., and N.K. Robakis. 1999. Presenilin-1 forms complexes with the cadherin/catenin cell–cell adhesion system and is recruited to intercellular and synaptic contacts. *Mol. Cell*. 4:893–902.

Guo, Q., B.L. Sopher, K. Furukawa, D.G. Pham, N. Robinson, G.M. Martin, and M.P. Mattson. 1997. Alzheimer's presenilin mutation sensitizes neural cells to apoptosis induced by trophic factor withdrawal and amyloid b-peptide: involvement of calcium and oxyradicals. *J. Neurosci.* 17:4212–4222.

Haass, C., and B. De Strooper. 1999. The presenilins in Alzheimer's disease—proteolysis holds the key. *Science*. 286:916–919.

Hardy, J. 1997. Amyloid, the presenilins and Alzheimer's disease. *Trends Neurosci.* 20:154–159.

Herreman, A., D. Hartmann, W. Annaert, P. Saftig, K. Craessaerts, L. Serneels, L. Umans, V. Schrijvers, F. Checler, H. Vanderstichele, et al. 1999. Presenilin-2 deficiency causes a mild pulmonary phenotype and no changes in amyloid precursor protein processing but enhances the embryonic lethal phenotype of presenilin-1 deficiency. *Proc. Natl. Acad. Sci. USA*. 96:11872–11877.

Hofmann, K., and P. Bucher. 1996. The UBA domain: a sequence motif present in multiple enzyme classes of the ubiquitination pathway. *Trends Biochem. Sci*. 21:172–173.

Honda, T., K. Yasutake, N. Nihonmatsu, M. Mercken, H. Takahashi, O. Murayama, M. Murayama, K. Sato, A. Omori, S. Tsubuki, T.C. Saido, and A. Takashima. 1999. Dual roles of proteasome in the metabolism of presenilin-1. *J. Neurochem*. 72:255–261.

Jacobsen, H., D. Reinhardt, M. Brockhaus, D. Bur, C. Kocyba, H. Kurt, M.G. Grim, R. Baumeister, and H. Loetscher. 1999. The influence of endoproteolytic processing of familial Alzheimer's disease presenilin 2 on Aβ42

amyloid peptide formation. *J. Biol. Chem.* 274:35233–35239.
Janicki, S., and M.J. Monteiro. 1997. Increased apoptosis arising from increased expression of the Alzheimer's disease-associated presenilin-2 mutation (N141I). *J. Cell Biol.* 139:485–495.
Janicki, S.M., and M.J. Monteiro. 1999. Presenilin overexpression arrests cells in the G1 phase of the cell cycle. Arrest potentiated by the Alzheimer's disease PS2(N141I) mutant. *Am. J. Pathol.* 155:135–144.
Johnston, J.A., C.L. Ward, and R.R. Kopito. 1998. Aggresomes: a cellular response to misfolded proteins. *J. Cell Biol.* 143:1883–1898.
Katayama, T., K. Imaizumi, N. Sato, K. Miyoshi, T. Kudo, J. Hitomi, T. Morihara, T. Yoneda, F. Gomi, Y. Mori, et al. 1999. Presenilin-1 mutations downregulate the signalling pathway of the unfolded-protein response. *Nat. Cell Biol.* 1:479–485.
Kaye, F.J., S. Modi, I. Ivanovska, E.V. Koonin, K. Thress, A. Kubo, S. Kornbluth, and M.D. Rose. 2000. A family of ubiquitin-like proteins binds the ATPase domain of Hsp70-like Stch. *FEBS Lett.* 467:348–355.
Kehoe, P., F. Wavrant-De Vrieze, R. Crook, W.S. Wu, P. Holmans, I. Fenton, G. Spurlock, N. Norton, H. Williams, N. Williams, et al. 1999. A full genome scan for late onset Alzheimer's disease. *Hum. Mol. Genet.* 8:237–245.
Kim, T.W., W.H. Pettingell, O.G. Hallmark, R.D. Moir, W. Wasco, and R.E. Tanzi. 1997. Endoproteolytic cleavage and proteasomal degradation of presenilin-2 in transfected cells. *J. Biol. Chem.* 272:11006–11010.
Kleijnen, M.F., A.H. Shih, P. Zhou, S. Kumar, R.E. Soccio, N.L. Kedersha, G. Gill, and P.M. Howley. 2000. The hPLIC proteins may provide a link between the ubiquitination machinery and the proteasome. *Mol. Cell* 6:409–419.
Kovacs, D.M., H.J. Fausett, K.J. Page, T.W. Kim, R.D. Moir, D.E. Merriam, R.D. Hollister, O.G. Hallmark, R. Mancini, K.M. Felsenstein, et al. 1996. Alzheimer-associated presenilins 1 and 2: neuronal expression in brain and localization to intracellular membranes in mammalian cells. *Nat. Med.* 2:224–229.
Krobitsch, S., and S. Lindquist. 2000. Aggregation of huntingtin in yeast varies with the length of the polyglutamine expansion and the expression of chaperone proteins. *Proc. Natl. Acad. Sci. USA.* 97:1589–1594.
Leissring, M.A., I. Parker, and F.M. LaFerla. 1999. Presenilin-2 mutations modulate amplitude and kinetics of inositol 1,4,5-trisphosphate-mediated calcium signals. *J. Biol. Chem.* 274:32535–32538.
Levitan, D., and I. Greenwald. 1995. Facilitation of lin-12-mediated signalling by sel-12, a *Caenorhabditis elegans* S182 Alzheimer's disease gene. *Nature.* 377:351–354.
Mattson, M.P., Q. Guo, K. Furukawa, and W.A. Pedersen. 1998. Presenilins, the endoplasmic reticulum, and neuronal apoptosis in Alzheimer's disease. *J. Neurochem.* 70:1–14.
Mical, T.I., and M.J. Monteiro. 1998. The role of sequences unique to nuclear intermediate filaments in the targeting and assembly of human lamin B: evidence for lack of interaction of lamin B with its putative receptor. *J. Cell Sci.* 111:3471–3485.
Monteiro, M.J., and T.I. Mical. 1996. Resolution of kinase activities during the HeLa cell cycle: identification of kinases with cyclic activities. *Exp. Cell Res.* 223:443–451.
Mori, H., J. Kondo, and Y. Ihara. 1987. Ubiquitin is a component of paired helical filaments in Alzheimer's disease. *Science.* 235:1641–1644.
Niwa, M., C. Sidrauski, R.J. Kaufman, and P. Walter. 1999. A role for presenilin-1 in nuclear accumulation of Ire1 fragments and induction of the mammalian unfolded protein response. *Cell.* 99:691–702.
Perry, G., R. Friedman, G. Shaw, and V. Chau. 1987. Ubiquitin is detected in neurofibrillary tangles and senile plaque neurites of Alzheimer disease brains. *Proc. Natl. Acad. Sci. USA.* 84:3033–3036.
Pickart, C.M. 1998. Polyubiquitin chains. *In* Ubiquitin and the Biology of the Cell. J.-M. Peters, J. R. Harris, and D. Finley, editors. Plenum Press, New York. 19–63.
Price, D.L., R.E. Tanzi, D.R. Borchelt, and S.S. Sisodia. 1998. Alzheimer's disease: genetic studies and transgenic models. *Annu. Rev. Genet.* 32:461–493.
Qian, S., P. Jiang, X.M. Guan, G. Singh, M.E. Trumbauer, H. Yu, H.Y. Chen, L.H. Van de Ploeg, and H. Zheng. 1998. Mutant human presenilin-1 protects presenilin-1 null mouse against embryonic lethality and elevates Ab1-42/43 expression. *Neuron.* 20:611–617.
Raina, A.K., M.J. Monteiro, A. McShea, and M.A. Smith. 1999. The role of cell cycle-mediated events in Alzheimer's disease. *Int. J. Exp. Pathol.* 80:71–76.
Shen, J., R.T. Bronson, D.F. Chen, W. Xia, D.J. Selkoe, and S. Tonegawa. 1997. Skeletal and CNS defects in presenilin-1-deficient mice. *Cell.* 89:629–639.
Stabler, S.M., L.L. Ostrowski, S.M. Janicki, and M.J. Monteiro. 1999. A myristoylated calcium-binding protein that preferentially interacts with the Alzheimer's disease presenilin-2 protein. *J. Cell Biol.* 145:1277–1292.
Steiner, H., H. Romig, M.G. Grim, U. Philipps, B. Pesold, M. Citron, R. Baumeister, and C. Haass. 1999. The biological and pathological function of the presenilin-1 Δexon 9 mutation is independent of its defect to undergo proteolytic processing. *J. Biol. Chem.* 274:7615–7618.
Sternberger, L.A. 1986. Immunochemistry. 3rd ed. John Wiley & Sons, Inc., New York. 524 pp.
Struhl, G., and I. Greenwald. 1999. Presenilin is required for activity and nuclear access of Notch in *Drosophila*. *Nature.* 398:522–525.
Warrick, J.M., H.Y. Chan, G.L. Gray-Board, Y. Chai, H.L. Paulson, and N.M. Bonini. 1999. Suppression of polyglutamine-mediated neurodegeneration in *Drosophila* by the molecular chaperone HSP70. *Nat.Genet.* 23:425–428.
Wong, P.C., H. Zheng, H. Chen, M.W. Becher, D.J. Sirinathsinghji, M.E. Trumbauer, H.Y. Chen, D.L. Price, L.H. Van der Ploeg, and S.S. Sisodia. 1997. Presenilin-1 is required for Notch1 and DII1 expression in the paraxial mesoderm. *Nature.* 387:288–292.
Wu, A.L., J. Wang, A. Zheleznyak, and E.J. Brown. 1999. Ubiquitin-related proteins regulate interaction of vimentin intermediate filaments with the plasma membrane. *Mol. Cell.* 4:619–625.
Ye, Y., N. Lukinova, and M.E. Fortini. 1999. Neurogenic phenotypes and altered Notch processing in *Drosophila* presenilin mutants. *Nature.* 398:525–529.